Biochemistry

© Copyright 1997 by the American Chemical Society Volume 36, Number 6 February 11, 1997

Accelerated Publications

Redox-Dependent Structural Changes in the Nitrogenase P-Cluster[†,‡]

John W. Peters,[§] Michael H. B. Stowell,[§] S. Michael Soltis,[∥] Michael G. Finnegan,[⊥] Michael K. Johnson,[⊥] and Douglas C. Rees*[,§]

Division of Chemistry and Chemical Engineering, 147-75CH, California Institute of Technology, Pasadena, California 91125, Stanford Synchrotron Radiation Laboratory, SLAC, P.O. Box 4249, Bin 69, Stanford University, Palo Alto, California 94309, and Department of Chemistry and Center for Metalloenzyme Studies, University of Georgia, Athens, Georgia 30602

Received October 24, 1996[⊗]

ABSTRACT: The structure of the nitrogenase MoFe-protein from *Azotobacter vinelandii* has been refined to 2.0 Å resolution in two oxidation states. EPR studies on the crystals indicate that the structures correspond to the spectroscopically assigned oxidized (P^{OX}/M^{OX}) and the native or dithionite-reduced (P^{N}/M^{N}) forms of the enzyme. Both MoFe-protein structures are essentially identical, with the exception of the P-cluster. The MoFe-protein P-cluster in each state is found to contain eight Fe and seven S atoms. Interconversion between the two redox states involves movement of two Fe atoms and an exchange of protein coordination for ligands supplied by a central S atom. In the oxidized P^{OX} state, the cluster is coordinated by the protein through six cysteine ligands, Ser-β188 Oγ, and the backbone amide of Cys-α88. In the native P^{N} state, Ser-β188 Oγ and the amide N of Cys-α88 no longer coordinate the cluster due to movement of their coordinated Fe atoms toward the central sulfur. Consequently, this central sulfur adopts a distorted octahedral environment with six surrounding Fe atoms. A previously described model of the P-cluster containing 8Fe-8S likely reflects the inappropriate modeling of a single structure to a mixture of these two P-cluster redox states. These observed redox-mediated structural changes of the P-cluster suggest a role for this cluster in coupling electron transfer and proton transfer in nitrogenase.

The reduction of dinitrogen to ammonia in biological systems is catalyzed by nitrogenase [recently reviewed in Peters et al. (1995a), Burgess and Lowe (1996), Eady (1996), Howard and Rees (1996), Muchmore et al. (1996), and Thorneley and Lowe (1996)]. Molybdenum-containing nitrogenase is composed of two separable components commonly referred to as the Fe-protein and MoFe-protein, indicating the content of their respective metal-containing prosthetic groups. During catalysis, these two components act in concert to transfer electrons from the Fe-protein to the MoFe-protein, where substrate reduction occurs. This process involves the hydrolysis of two MgATP molecules per electron transferred in a reaction that can be represented by the following limiting stoichiometry:

$$N_2 + 8H^+ + 8e^- + 16MgATP \rightarrow 2NH_3 + H_2 + 16MgADP + 16P_i$$

The X-ray crystal structures of both the Fe-protein and the

[†] This work was supported by NSF DMB 91-18689 (D.C.R.), NIH GM51962 (M.K.J.), and an NIH postdoctoral fellowship (GM18142) to J.W.P. The rotation camera facility at the Stanford Synchrotron Radiation Laboratory is supported by the DOE Office of Basic Energy Sciences and the NIH Biomedical Technology Program, Division of Research Resources.

[‡] Coordinates for the P^{OX}/M^{OX} and P^{N}/M^{N} states of the nitrogenase MoFe−protein are deposited in the Brookhaven Protein Data Bank and assigned the ID codes 2MIN and 3MIN, respectively.

* To whom correspondence should be addressed. Telephone: (818)-395-8393. Fax: (818)-584-6785. E-mail: rees@citray.caltech.edu.

[§] California Institute of Technology.

[∥] Stanford University.

[⊥] University of Georgia.

[⊗] Abstract published in *Advance ACS Abstracts,* January 15, 1997.

S0006-2960(96)02666-9 CCC: $14.00 © 1997 American Chemical Society

MoFe-protein have been determined from the free-living nitrogen-fixing microorganism *Azotobacter vinelandii* (Georgiadis et al., 1992; Kim & Rees, 1992a,b; Muchmore, 1995) and the obligate anaerobe *Clostridium pasteurianum* (Bolin et al., 1993; Kim et al., 1993; Campobasso, 1994; Woo, 1995). The nitrogenase Fe-protein exists as a dimer of identical subunits bridged by a single 4Fe-4S cubane. Structural and sequence comparisons place the Fe-protein in a large class of proteins in which energy from the binding and hydrolysis of nucleotide triphosphates is coupled to changes in protein conformation. In the nitrogenase system, these conformational changes are used to drive electron transfer from the 4Fe-4S cluster of the Fe-protein to the substrate reduction site of the MoFe-protein. The MoFe-protein is an $\alpha_2\beta_2$–tetramer that contains two types of metalloclusters, the FeMo-cofactor and the P-cluster. Each $\alpha\beta$-dimer is thought to function as an independent half and contains one FeMo-cofactor, or M center, and one P-cluster. The FeMo-cofactor is located entirely within the α-subunit and is the site of substrate binding and reduction. The P-cluster is located at the interface of the α- and β-subunits, and it is believed to participate in the transfer of electrons from the Fe-protein to the substrate reduction site. During catalysis, the Fe-protein dimer docks with an $\alpha\beta$-dimer, followed by electron transfer coupled to the hydrolysis of two MgATP, with subsequent dissociation of the protein complex. The reduction of a single molecule of dinitrogen requires multiple electron transfer events, and dissociation of the complex likely represents the rate-limiting step during turnover.

There are several lines of indirect evidence, including data from mutagenesis studies (Peters et al., 1995b; May et al., 1991) and kinetic measurements (Lowe et al., 1993), that the P-cluster does indeed serve as an intermediary in electron transfer from the 4Fe-4S cluster of the Fe-protein to the FeMo-cofactor at the substrate reduction site. The redox properties of the P-cluster are of great interest in view of the electron transfer function of this center. Mössbauer studies on the dithionite-reduced state or native state (P^N) indicate that all the iron atoms in the cluster are in the ferrous state (Surerus et al., 1992). While more reduced forms of the P-cluster (if they exist) have not yet been detected, several oxidized forms have been identified, including a two-electron-oxidized form designated P^{OX} (Zimmerman et al., 1978) that can be reversibly generated from P^N. Under conditions where the FeMo-cofactor has been oxidized by one-electron from the M^N to the M^{OX} state, the P-cluster is oxidized to at least the P^{OX} state (Pierik et al., 1993).

There has been some controversy about the composition and structure of the P-cluster, specifically concerning the number and bonding arrangements of S atoms in this cluster. While there is general agreement that the P-cluster contains eight Fe atoms, models of the P-cluster with either eight S or seven S have been proposed. In the 8Fe-8S model, the P-cluster has been described as a pair of 4Fe-4S cubanes bridged by a disulfide bond formed between cluster sulfur atoms in each cubane (Chan et al., 1993). Two versions of a 8Fe-7S P-cluster have been described that can be formally derived from the 8Fe-8S model by removal of one of the sulfur atoms in the disulfide bond. In one model, first discussed by Bolin et al. (1993) and detailed by Campobasso (1994) and Muchmore (1994), the P-cluster may be formally considered to consist of two 4Fe-3S partial cubanes bridged by a single hexacoordinate S bound equivalently by each partial cubane. A second 8Fe-7S form has also been suggested that can be generated, at least formally, from bridged 4Fe-4S and 4Fe-3S clusters (Chan et al., 1993). It has been proposed that differences in these models may reflect, at least in part, different oxidation states of the P-cluster (Rees, 1993).

Table 1: Data and Refinement Statistics

	oxidized	reduced
Data Statistics		
a (Å)	107.7	108.0
b (Å)	130.2	131.3
c (Å)	81.3	81.0
β (deg)	110.8	110.7
resolution range (Å)	30.0−2.0	30.0−2.0
observations	563 832	576 617
unique reflections	125 947	125 145
R_{merge} (%)	8.2 (17.3)[a]	5.8 (16.2)[a]
completeness (%)	93.4 (83.8)[a]	92.0 (77.1)[a]
Refinement Statistics		
resolution range (Å)	30.0−2.0	30.0−2.0
total reflections ($F > 1\sigma F$)	123 552	121 909
R_{cryst}	0.211	0.206
R_{free}	0.267	0.264
rms of bond distances (Å)	0.015	0.016
rms of angles (deg)	2.88	2.88

[a] Statistics for the highest-resolution shell (2.06−2.03 Å) are indicated in parentheses. $R_{merge} = \sum_{hkl}[\sum_i(|I_{hkl,i} - \langle I_{hkl}\rangle|)]/\sum_{hkl,i}\langle I_{hkl}\rangle$, where I_{hkl} is the intensity of an individual measurement of the reflection with indices *hkl* and $\langle I_{hkl}\rangle$ is the mean intensity of that reflection.

In this paper, we address these issues concerning the structure of the P-cluster and the possible variation in P-cluster structure with oxidation state, through determination at 2.0 Å resolution of the structure of the *A. vinelandii* MoFe-protein in oxidized (P^{OX}/M^{OX}) and dithionite-reduced (P^N/M^N) states.

METHODS

Wild-type *A. vinelandii* was cultured at 25−30 °C in modified, liquid Burke media (Strandberg & Wilson, 1968). Large scale growth was accomplished using 20 L carboys and monitored using a Hewlett-Packard 8453 UV-Visible spectrophotometer. The *A. vinelandii* MoFe-protein was purified as described previously (Burgess et al., 1980) with modifications described in Peters et al. (1994); however, the final hydrophobic interaction (phenyl-sepharose) step was substituted by gel filtration with Sephacyl-200. The purification was accomplished under anaerobic conditions, using 1 mM sodium dithionite as the reducing agent to remove residual oxygen from buffers. During gel filtration chromatography, the MoFe-protein was equilibrated with 0.35 M NaCl, 25 mM Tris (pH 8.5), 20% glycerol, and 1 mM dithionite. SDS−PAGE (Laemmli, 1970) was used to monitor the purification and indicated that the protein was greater than 90% pure.

The MoFe-protein was crystallized by microcapillary batch diffusion using 30% PEG 8000, 0.2 M $NaMoO_4$, and 0.1 M Tris (pH 8.5) as precipitating solution (Kim & Rees, 1992b). The MoFe-protein crystals are dark brown in color and grow in 1−1.5 months to an average size of $0.1 \times 0.3 \times 0.8$ mm^3 in space group $P2_1$ with unit cell parameters (Table 1) similar to those described in Kim and Rees (1992b). Methylviologen paper was used as an indicator of the reducing state of the crystallization mother liquor after the 1−1.5 month crystal

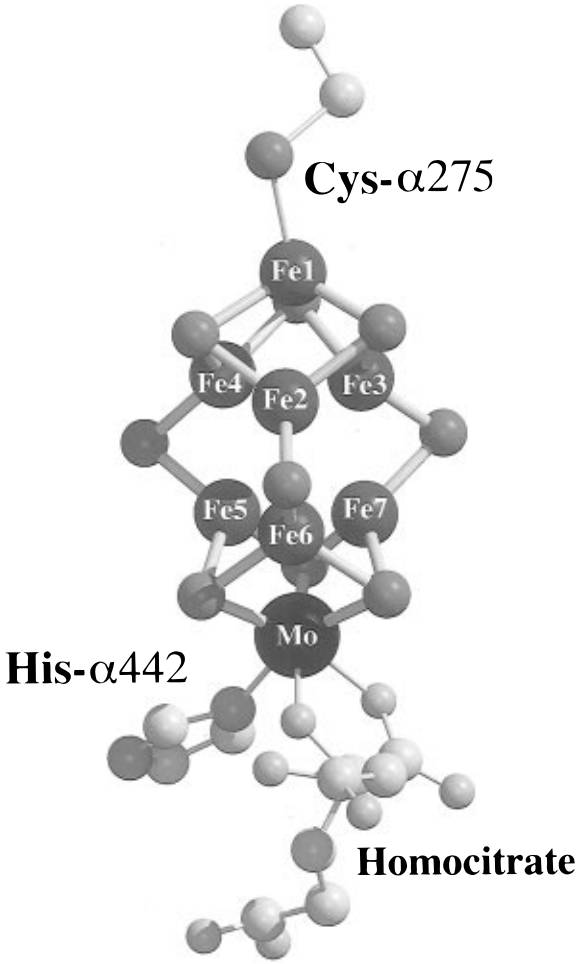

FIGURE 1: FeMo-cofactor model. Fe atoms and Mo are labeled and shown in dark gray and black, respectively, and are numbered as they appear in the text and in Table 2. All sulfur atoms and the nitrogen atoms of His-α442 are shown in medium gray. Carbon and oxygen atoms of the homocitrate moiety are shown in light gray.

growth period. MoFe-protein crystals were assayed for nitrogenase acetylene reduction activity at 30 °C in 9 mL Wheaton vials fitted with butyl rubber stoppers and aluminum crimp seals. Several crystals were resuspended in 25 mM Tris (pH 7.4) and 1 mM sodium dithionite buffer. Each assay (1 mL) included a MgATP-regenerating system containing 30 units of creatine phosphokinase, 30 mM phosphocreatine, 2.5 mM ATP, and 5 mM $MgCl_2$ in 25 mM HEPES (pH 7.4). Sodium dithionite was used as a reductant at a final concentration of 20 mM. The gas chromatograph was calibrated using standards containing 1000 ppm ethylene (Scott Specialty Gases, Durham, NC). Ethylene was analyzed using a Varian model 3700 gas chromatograph using a fused silica capillary column equipped with a flame ionization detector. Nitrogenase MoFe-protein activity was determined at a saturating ratio of purified Fe-protein to MoFe-protein. Protein concentrations were determined by the method of Lowry et al. (1951).

MoFe-protein crystals were cryopreserved at approximately −180 °C prior to data collection. The crystals were flash cooled in liquid nitrogen on rayon loops, and data were collected under a continuous nitrogen stream at approximately −180 °C. Data were collected on a MAR imaging plate detector on beam-line 7-1 ($\lambda = 1.08$ Å) at the Stanford Synchrotron Radiation Laboratory. The data were processed using DENZO and SCALEPACK (Otwinowski, 1993), and the structures were refined in parallel with X-PLOR (Brünger et al., 1987) using the protein parameters of Engh and Huber (1991). The quality of the refined structures was analyzed using PROCHECK (Laskowski et al., 1993). All structural figures were produced using the programs MOLSCRIPT (Kraulis, 1991) and RASTER3D (Bacon & Anderson, 1988; Merritt & Murphy, 1994).

X-band EPR spectra were recorded on a Bruker ESP-300E EPR spectrometer with a dual-mode ER-4116 cavity and equipped with an Oxford Instruments ESR-9 flow cryostat. A single crystal of nitrogenase MoFe-protein in a quartz capillary tube was placed inside X-band EPR tubes and adhered to the side with a drop of water in the vicinity of the crystal to ensure anchoring and good thermal contact on freezing. Dithionite reduction was carried out by thawing the EPR sample in a Vacuum Atmospheres glovebox under argon (<1 ppm O_2), adding a small crystal of dithionite to the mother liquor surrounding the crystal, and refreezing after incubation at room temperature for 15 min.

RESULTS AND DISCUSSION

The structure of the nitrogenase MoFe-protein from *A. vinelandii* has been refined to 2.0 Å resolution in two states: in the as-crystallized form and after reduction with dithionite. Details of the X-ray diffraction data and the respective structure refinement are shown in Table 1. The as-crystallized and dithionite-reduced states of the MoFe-protein have been refined to an R_{cryst} of 0.211 and 0.206, respectively. At this stage of refinement, each model has 88% of its atoms in most-favored regions of the Ramachandran diagram, with less than 0.2% outliers (Laskowski et al., 1993).

Several lines of evidence indicate that the MoFe-protein as crystallized corresponds to an oxidized (P^{OX}/M^{OX}) state, while the dithionite-reduced state corresponds to a more reduced form that is equivalent to the native or as-isolated state (P^N/M^N). First, the mother liquor surrounding the crystals was not reducing to methylviologen paper when checked just prior to data collection. It is therefore likely that the dithionite in the mother liquor was consumed over the time course of crystallization (1−1.5 months). Second, single-crystal EPR studies showed no resonances in either parallel or perpendicular mode over the temperature range of 4.2−10 K. Not observing a resonance attributable to the $S = {}^3/_2$ FeMo-cofactor center in the M^N state indicates that this cluster is oxidized to the diamagnetic M^{OX} state, which dictates that the P-cluster must at least be oxidized to the first P^{OX} state (Pierik et al., 1993). The absence of any resonances attributable to either an $S = {}^1/_2$ or ${}^7/_2$ spin system suggests that the P-cluster is in the $S = 3$ or 4 P^{OX} state. This state does exhibit a weak parallel- and perpendicular-mode EPR signal at $g = 12$, but this resonance is difficult to observe even in highly concentrated solution samples (Pierik et al., 1993; Surerus et al., 1992) and would be expected to be difficult, if not impossible, to observe for a single-crystal sample. On dissolution, the oxidized crystals were found to be active in nitrogenase acetylene reduction assays, having a specific activity of approximately 1800 nmol of acetylene formed per minute per milligram of MoFe-protein. This activity is on the order of that observed for highly active MoFe-protein, indicating that the sample has

Table 2: Metal−Metal Distances in the M^{OX} and M^{N} States of the FeMo-Cofactor (in Angstroms)[a]

	Fe1	Fe2	Fe3	Fe4	Fe5	Fe6	Fe7	Mo1
Fe1		2.62	2.58	2.65	4.93	4.89	4.89	6.89
Fe2	2.69 (+0.07)		2.57	2.62	3.62	2.51	3.58	4.96
Fe3	2.73 (+0.15)	2.67 (+0.10)		2.56	3.58	3.54	2.53	4.95
Fe4	2.74 (+0.09)	2.67 (+0.05)	2.65 (+0.09)		2.55	3.63	3.63	5.01
Fe5	5.04 (+0.11)	3.70 (+0.08)	3.66 (+0.08)	2.55 (0.00)		2.57	2.56	2.69
Fe6	4.98 (+0.09)	2.54 (+0.03)	3.64 (+0.10)	3.63 (0.00)	2.60 (+0.03)		2.46	2.64
Fe7	5.07 (+0.18)	3.65 (+0.07)	2.63 (+0.10)	3.68 (+0.05)	2.55 (−0.01)	2.47 (+0.01)		2.63
Mo1	7.01 (+0.12)	5.00 (+0.04)	5.00 (+0.05)	5.03 +0.02)	2.74 (+0.05)	2.65 (+0.01)	2.54 (−0.09)	

[a] Distances between pairs of metal atoms are indicated for the M^{N} state (upper right) and M^{OX} state (lower left). The distances are the average of the two FeMo-cofactors in the crystallographic asymmetric unit of the *A. vinelandii* MoFe-protein. The average deviation between crystallographically independent metal−metal distances is 0.06 Å, with a maximum of 0.13 Å for the Fe4−Fe6 pair. The numbers in parentheses in the lower left indicate the change in average metal−metal distance upon oxidation of M^{N} to M^{OX}.

not been irreversibly oxidized. Data from the crystal assigned to the P^{N}/M^{N} state were collected on the same batch of crystals after adding 10 mM dithionite to the mother liquor and incubating overnight. The mother liquor from these crystals did reduce methyl viologen paper. Moreover, dithionite reduction of the single-crystal sample used for EPR studies resulted in a sample exhibiting a resonance at 10 K indicative of the $S = {}^{3}/_{2}$ FeMo-cofactor center in the M^{N} state. The resonance comprises a broad derivative that varies in both intensity and crossover position ($g = 3.2-2.6$) as the crystal is rotated by 360° in the cavity. Such behavior is indicative of 360° rotation of a randomly oriented single crystal of an $S = {}^{3}/_{2}$ paramagnet with $g = 4.32$, 3.68, and 2.01 as the principle components of the **g** tensor for the lowest doublet (Gurbiel et al., 1991).

The FeMo-cofactor structure (Figure 1) in either the M^{OX} or M^{N} state is consistent with the overall geometry and coordination environment of that previously described (Kim & Rees, 1992a,b; Chan et al., 1993). The relevant refined metal−metal distances shown in Table 2 compare well to distances derived from Fe and Mo EXAFS (Chen et al., 1993). There is an indication of a slight decrease in the Fe−Mo and Fe−Fe distances on going from the M^{OX} to the M^{N} state, especially within the 4Fe-3S partial cubane (Table 2). Although these changes are less than the estimated coordinate error, they are consistent with results of EXAFS studies in which shorter metal−metal distances are observed on reduction of the MoFe-protein (Christiansen et al., 1995).

The most significant differences in the structures of the P^{OX}/M^{OX} and P^{N}/M^{N} states of the MoFe-protein are restricted to the P-cluster. The P-cluster in either oxidation state is an 8Fe-7S cluster (Figures 2 and 3). In the oxidized state, the P-cluster may be described as one containing bridged 4Fe-4S and 4Fe-3S clusters that are predominantly bound to the α- and β-subunits, respectively. In this form, the central sulfur of the P-cluster, designated S1 in Figure 2, is four-coordinate, as it is within bonding distance to three Fe atoms of the α-subunit cubane and one Fe atom of the β-subunit partial cubane. Upon reduction to P^{N}, an additional Fe atom (Fe5 in Figure 2) of the β-subunit partial cubane moves within bonding distance of S1, while Fe6 moves to within 3 Å of S1. As a result of these changes, the S1 sulfur is surrounded by a distorted octahedral arrangement of six

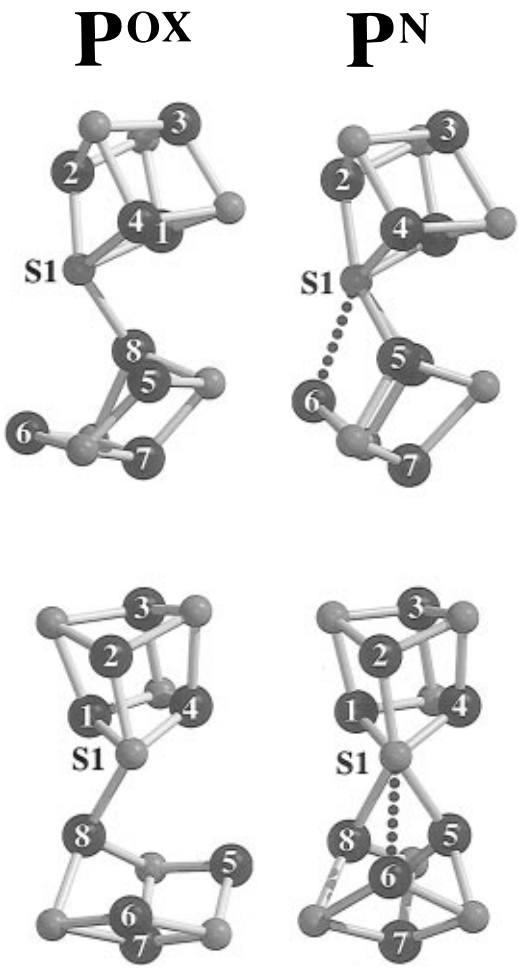

FIGURE 2: Structural models of the P^{N} and P^{OX} of the P-cluster viewed from two perpendicular directions. Fe atoms are shown in black and are numbered as they appear in the text and in Table 3. Sulfur atoms are shown in light gray. The bonding of the central sulfur (S1) to Fe6 is shown as a dotted line because the S1−Fe6 distance (2.92 Å) is longer than the normal Fe−S bond distance.

iron atoms in P^{N}. The resulting P-cluster structure resembles that first described by Bolin and co-workers (Bolin et al., 1993; Campobasso, 1994; Muchmore, 1995), and more recently in the *Klebsiella pneumoniae* MoFe-protein (D. Lawson, S. M. Roe, C. Gorman, and B. E. Smith, personal communication). The Fe−Fe and Fe−S1 distances in the

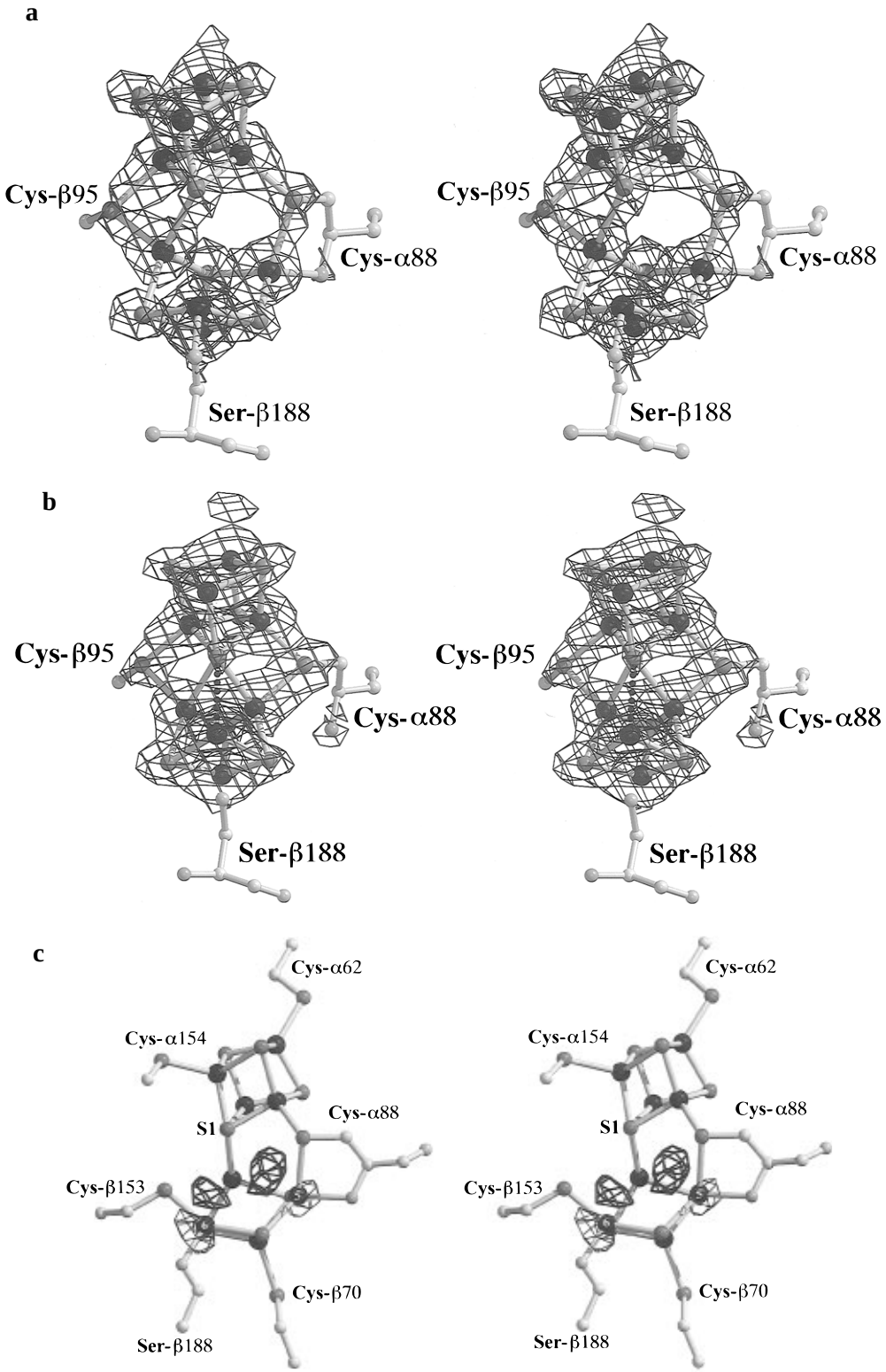

FIGURE 3: Stereoview of $2F_o - F_c$ electron density maps calculated at 2 Å resolution with the final refined models for (a) P^{OX} and (b) P^N. The electron density map is contoured at 3.5σ. (c) Stereoview of the $F_o - F_o$ (reduced − oxidized) difference electron density maps showing the differences in the vicinity of the P-cluster. The model for the P^{OX} form of the P-cluster is illustrated, with the Fe coordination by Ser-β188 and Cys-α88 indicated. Positions of Fe5 and Fe6 in the P^N appear as positive density (8σ) and are shown in bold contour, while the corresponding positions of these Fe atoms in the P^{OX} state appear as negative density (-9σ) and are shown by thin lines.

P^{OX} and P^N states are summarized in Table 3.

Redox-mediated structural changes in the P-cluster are dominated by movement of two of the four Fe atoms of the β-subunit partial cubane. From their positions in the P^{OX} state, Fe5 and Fe6 move 1.4 and 0.9 Å, respectively, toward the central sulfur in the P^N state (Figure 2, Table 3). The movement of Fe5 and Fe6 upon reduction to P^N contributes to an overall decrease in the average MoFe-protein Fe−Fe distance of 0.25 Å from 3.89 to 3.64 Å. These changes are consistent with EXAFS studies that indicate contraction of metal−metal distances on reduction (Christiansen et al., 1995). These differences between the P^{OX} and P^N states are evident in a difference electron density map calculated between the observed data sets for these two redox states

Table 3: Metal−Metal and Metal−Sulfur S1 Distances in the P^{OX} and P^{N} States of the P-Cluster (in Angstroms)[a]

	Fe1	Fe2	Fe3	Fe4	Fe5	Fe6	Fe7	Fe8	S1
Fe1		2.42	2.70	2.53	3.77	4.76	5.42	3.05	2.26
Fe2	2.43 (+0.01)		2.76	2.54	4.59	5.02	6.64	4.46	2.34
Fe3	2.71 (+0.01)	2.78 (+0.02)		2.59	5.37	6.83	7.61	5.57	3.97
Fe4	2.48 (−0.05)	2.61 (+0.07)	2.69 (+0.10)		3.03	4.70	5.57	4.06	2.23
Fe5	4.80 (+1.03)	5.78 (+1.19)	6.23 (+0.86)	3.77 (+0.74)		2.56	2.66	2.46	2.43
Fe6	5.72 (+0.94)	6.07 (+1.05)	7.90 (+1.07)	5.64 (+0.94)	3.88 (+1.32)		2.65	2.52	2.92
Fe7	5.43 (+0.01)	6.76 (+0.12)	7.69 (+0.08)	5.57 (0.0)	2.76 (+0.10)	2.77 (+0.12)		2.62	4.31
Fe8	2.96 (+0.09)	4.37 (+0.11)	5.51 (−0.06)	3.89 (+0.17)	3.41 (+0.95)	3.22 (+0.70)	2.72 (+0.10)		2.45
S1	2.27 (+0.01)	2.30 (−0.04)	4.06 (+0.09)	2.26 (+0.03)	3.81 (+1.38)	3.86 (+0.94)	4.42 (+0.11)	2.32 (−0.13)	

[a] Distances between pairs of metal atoms are indicated for the P^{N} state (upper right) and P^{OX} state (lower left). The distances are the average of the two P-clusters in the crystallographic asymmetric unit of the *A. vinelandii* MoFe-protein. The average deviation between crystallographically independent metal−metal distances is 0.05 Å, with a maximum of 0.11 Å for the Fe1−Fe6 pair in P^{N}. The numbers in parantheses in the lower left indicate the change in average distance upon oxidation of P^{N} to P^{OX}.

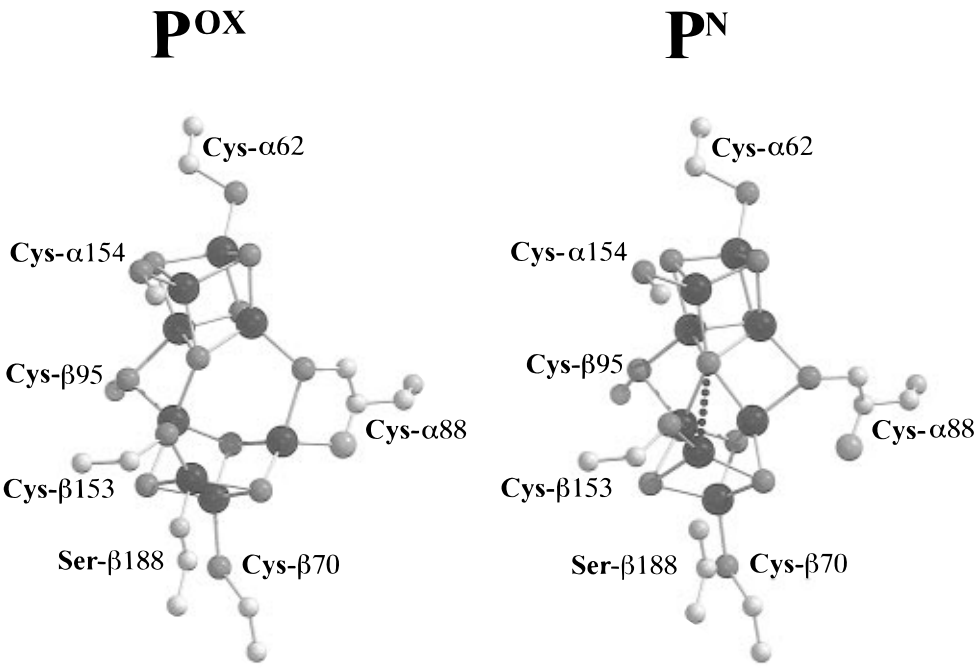

FIGURE 4: Comparison of the P-cluster structures in the P^{OX} and P^{N} states. For clarity, the cluster is depicted with the same orientation and shading scheme as the two views shown in Figure 2.

(Figure 3c). With the exception of Fe5 and Fe6, other atoms in the P-cluster show little change between P^{OX} and P^{N}, as shown by the absence of any substantial difference density in any area of the P-cluster other than near these two Fe atoms (Figure 3c).

Previously, an 8Fe-8S model for the P-cluster was proposed that could be formally considered as being generated from two 4Fe-4S clusters linked by a disulfide bridge (Chan et al., 1993; Rees, 1993). Using crystals of the MoFe-protein characterized with respect to oxidation state and activity, however, we found no evidence in the present study for either eight sulfurs or a disulfide bridge in the P-cluster. Since a superposition of the P^{N} and P^{OX} structures qualitatively resembles that expected for the proposed 8Fe-8S cluster, it appears likely that the latter was incorrectly proposed after modeling a single structure to a superposition of P^{N} and P^{OX} electron densities resulting from a mixture of the two types of 8Fe-7S clusters in our MoFe-protein crystals.

As previously described (Kim & Rees, 1992a,b), the P-cluster is covalently coordinated to the MoFe-protein through six cysteinyl ligands, three from the α-subunit and three from the β-subunit. Cys-α62 and Cys-α154 coordinate Fe3 and Fe2, respectively, while Cys-α88 provides a bridging cysteinyl ligand that coordinates both Fe4 and Fe5 (Figure 4). In an analogous manner, Cys-β70 and Cys-β153 coordinate Fe7 and Fe6, respectively, while Cys-β95 serves as a bridging ligand that binds both Fe1 and Fe8. Upon reduction of P^{OX} to P^{N}, movement of the Fe5 and Fe6 atoms within the P-cluster is accompanied by an exchange of covalent ligands. In the oxidized state, two additional protein ligands are present in addition to the cysteinyl ligands. Cys-α88 coordinates Fe5 with a backbone amide nitrogen ligand (in addition to providing a cysteinyl ligand to this same Fe), while the Oγ of Ser-β188 coordinates Fe6 (which is also

bound by the cysteinyl group of Cys-β153). The Ser-β188 side chain also interacts with a buried water molecule, although it is not clear whether the Oγ serves a proton donor or acceptor that would reflect the protonation state of the serine ligand. The Ser-β188 Oγ−Fe6 and -α88 N−Fe5 distances are on the average 1.99 and 2.17 Å, respectively, for the two crystallographically independent copies of the P^{OX} cluster. In the reduced state, these two noncysteinyl ligands are replaced by interactions with the central S1 sulfur (Figures 3 and 4). Hence, in both P^N and P^{OX}, all Fe in the P-cluster remain four-coordinate, although details of the coordination environments change with oxidation state.

Mutagenesis studies introducing single substitutions of the P-cluster cysteinyl ligands of the *A. vinelandii* MoFe-protein indicate that only Cys-α88 and Cys-β153 can tolerate replacement (Dean et al., 1990; May et al., 1991). These residues are involved in coordinating Fe5 and Fe6, respectively, which undergo the most substantial conformational changes between P^{OX} and P^N. Interestingly, these Fe are also coordinated by additional, noncysteinyl protein ligands in P^{OX}. Furthermore, substitution of Ser-β188 by Gly results in an altered MoFe with a biochemical phenotype similar to that of an altered MoFe-protein with Ser substituted for Cys-β153 (Peters et al., 1995a). Although the mechanistic significance of these observations is unclear, it is striking that replacement of residues that coordinate the Fe that vary most between P^N and P^{OX} can be achieved without complete disruption of nitrogenase activities.

The structural changes accompanying oxidation of the P-cluster raise the possibility that the P-cluster may be involved in coupling electron and proton transfer in nitrogenase. Oxidation of the P-cluster is accompanied by coordination of Ser-β188 and the amide nitrogen of Cys-α88 to cluster Fe atoms. Since both of these ligands will be protonated in their free states and may be deprotonated in their bound states, this raises the intriguing possibility that two-electron oxidation of the P-cluster simultaneously releases two protons. Transfer of electrons and protons to the FeMo-cofactor active site of nitrogenase needs to be synchronized, and the data presented in this paper suggest that the coupling of proton and electron transfer can also occur at the P-cluster. The observed ligand exchange mechanism may be utilized to enforce unidirectional electron flow through the P-cluster, by controlling protonation of the exchangeable ligands. Ultimately, ligand exchange at the P-cluster that couples proton and electron transfer in this system may be modulated during complex formation between the Fe-protein and the MoFe-protein. The structural complexity and redox-dependent structural changes of the P-cluster are unusual among characterized Fe-S clusters that are involved in electron transport and may well result from its ability to function in multiple roles.

ACKNOWLEDGMENT

Discussions with J. B. Howard are gratefully acknowledged.

REFERENCES

Bacon, D., & Anderson, W. F. (1988) *J. Mol. Graphics 6*, 219−220.

Bolin, J. T., Campobasso, N., Muchmore, S. W., Morgan, T. V., & Mortenson, L. E. (1993) in *Molybdenum Enzymes, Cofactors and Model Systems* (Stiefel, E. I., Coucouvanis, D., & Newton, W. E., Eds.) pp 186−195, American Chemical Society, Washington, DC.

Brünger, A. T., Kuriyan, J., & Karplus, M. (1987) *Science 235*, 458−460.

Burgess, B. K., & Lowe, D. J. (1996) *Chem. Rev. 96*, 2983−3011.

Burgess, B. K., Steifel, E. I., & Newton, W. E. (1980) *J. Biol. Chem. 255*, 353−356.

Campobasso, N. (1994) Ph.D. Dissertation, Purdue University, West Lafayette, IN.

Chan, M. K., Kim, J., & Rees, D. C. (1993) *Science 260*, 792−794.

Chen, J., Christiansen, J., Tittsworth, R. C., Hales, B. J., George, S. J., Coucouvanis, D., & Cramer, S. P. (1993) *J. Am. Chem. Soc. 115*, 5509−5515.

Christiansen, J., Tittsworth, R. C., Hales, B. J., & Cramer, S. P. (1995) *J. Am. Chem. Soc. 117*, 10017−10024.

Eady, R. R. (1996) *Chem. Rev. 96*, 3013−3030.

Engh, R. A., & Huber, R. (1991) *Acta Crystallogr. A47*, 392−400.

Georgiadis, M. M., Komiya, H., Chakrabarti, P., Woo, D., Kornuc, J. J., & Rees, D. C. (1992) *Science 257*, 1653−1659.

Gurbiel, R. J., Bolin, J. T., Ronco, A. E., Mortenson, L. E., & Hoffman, B. M. (1991) *J. Magn. Reson. 91*, 227−240.

Howard, J. B., & Rees, D. C. (1996) *Chem. Rev. 96*, 2965−2982.

Kim, J., & Rees, D. C. (1992a) *Nature 360*, 553−560.

Kim, J., & Rees, D. C. (1992b) *Science 257*, 1677−1682.

Kim, J., Woo, D., & Rees, D. C. (1993) *Biochemistry 32*, 7104−7115.

Kraulis, P. J. (1991) *J. Appl. Crystallogr. 24*, 946−950.

Laemmli, U. K. (1970) *Nature 227*, 680−685.

Laskowski, R. A., McArthur, M. W., Moss, D. S., & Thorton, J. M. (1993) *J. Appl. Crystallogr. 26*, 283−291.

Lowe, D. J., Fisher, K., & Thorneley, R. N. F. (1993) *Biochem. J. 292*, 93−98.

Lowry, O. H. (1951) *J. Biol. Chem. 193*, 265−275.

May, H. D., Dean, D. R., & Newton, W. E. (1991) *Biochem. J. 227*, 457−464.

Merritt, E. A., & Murphy, M. E. P. (1994) *Acta Crystallogr. D50*, 869−873.

Muchmore, S. W. (1995) Ph.D. Dissertation, Purdue University, West Lafayette, IN.

Muchmore, S. W., Jack, R. F., & Dean, D. R. (1996) *Adv. Inorg. Biochem. 11*, 111−133.

Otwinowski, Z. (1993) in *Data Collection and Processing* (Sawyer, L., Issacs, N., & Bailey, S., Eds.) pp 56−62, SERC Daresbury Laboratory, Daresbury, U.K.

Peters, J. W., Fisher, K., & Dean, D. R. (1994) *J. Biol. Chem. 269*, 28076−28083.

Peters, J. W., Fisher, K., & Dean, D. R. (1995a) *Annu. Rev. Microbiol. 49*, 335−366.

Peters, J. W., Fisher, K., Newton, W. E., & Dean, D. R. (1995b) *J. Biol. Chem. 270*, 27007−27013.

Pierik, A. J., Wassink, H., Haaker, H., & Hagen, W. R. (1993) *Eur. J. Biochem. 212*, 51−61.

Rees, D. C. (1993) *Curr. Opin. Struct. Biol. 3*, 921−928.

Strandberg, G. W., & Wilson, P. W. (1968) *Can. J. Microbiol. 14*, 25−31.

Surerus, K. K., Hendrich, M. P., Christie, P. D., Rottgardt, D., Orme-Johnson, W. H., & Münck, E. (1992) *J. Am. Chem. Soc. 114*, 8579−8590.

Thorneley, R. N. F., Lowe, D. J. (1996) *J. Biol. Inorg. Chem. 1*, 576−580.

Woo, D. (1995) Ph.D. Dissertation, University of California at Los Angeles, Los Angeles.

Zimmerman, R., Münck, E., Brill, W. J., Shah, V. K., Henzl, M. T., Rawlings, J., & Orme-Johnson, W. H. (1978) *Biochim. Biophys. Acta 537*, 185−207.

BI9626665